

Cite this: *Chem. Sci.*, 2017, **8**, 4123

Reactivity of hydride bridges in a high-spin $[\text{Fe}_3(\mu\text{-H})_3]^{3+}$ cluster: reversible H_2/CO exchange and $\text{Fe}-\text{H}/\text{B}-\text{F}$ bond metathesis†

Kevin J. Anderton,^a Brian J. Knight,^a Arnold L. Rheingold,^c Khalil A. Abboud,^b Ricardo García-Serres^d and Leslie J. Murray^a  

The triiron trihydride complex $\text{Fe}_3\text{H}_3\text{L}$ (**1**) [where L^{3-} is a tris(β -diketiminate)cyclophanate] reacts with CO and with $\text{BF}_3\cdot\text{OEt}_2$ to afford $(\text{Fe}^{\text{I}}\text{CO})_2\text{Fe}^{\text{II}}(\mu_3\text{-H})\text{L}$ (**2**) and $\text{Fe}_3\text{F}_3\text{L}$ (**3**), respectively. Variable-temperature and applied-field Mössbauer spectroscopy support the assignment of two high-spin (HS) iron(I) centers and one HS iron(II) ion in **2**. Preliminary studies support a CO-induced reductive elimination of H_2 from **1**, rather than CO trapping a species from an equilibrium mixture. This complex reacts with H_2 to regenerate **1** under a dihydrogen atmosphere, which represents a rare example of reversible CO/H_2 exchange and the first to occur at high-spin metal centers, as well as the first example of a reversible multielectron redox reaction at a designed high-spin metal cluster. The formation of **3** proceeds through a previously unreported net fluoride-for-hydride substitution, and **3** is surprisingly chemically inert to Si–H bonds and points to an unexpectedly large difference between the $\text{Fe}-\text{F}$ and $\text{Fe}-\text{H}$ bonds in this high-spin system.

Received 21st December 2016
Accepted 27th March 2017

DOI: 10.1039/c6sc05583d
rsc.li/chemical-science

Introduction

Beginning with Hieber's discovery of $\text{H}_2\text{Fe}(\text{CO})_4$ and $\text{HCo}(\text{CO})_4$,¹ the synthesis and reactivity studies of transition metal hydrides have remained an active area of chemical research.² Mononuclear metal hydrides have applications in industry (e.g., hydroformylation), electrocatalysis, and chemical synthesis.³ In addition, polynuclear transition metal hydrides have garnered substantial interest as these species have either been identified as or are proposed to be key intermediates in reactions in biological and chemical systems. For example, hydrides bound to iron centers are known or proposed in the Haber–Bosch⁴ and Fischer–Tropsch⁵ processes, dihydrogen oxidation/proton reduction by the nickel–iron and iron–iron hydrogenases,⁶ and the catalytic cycles for nitrogenases⁷ and nickel–iron carbon monoxide dehydrogenase.⁸ Molecular systems designed to model the multimetallic activation of H_2 to generate and probe

the reactivity of polynuclear metal hydrides generally use strong field donors (e.g., CO or phosphines).⁹ It remains unclear how parameters such as the metal coordination number and spin state tune reactivity of metal hydrides. This consideration is important in the context of heterogeneous and biological metal hydride clusters in which high- or intermediate-spin metal centers are typically present. The NiFe and FeFe hydrogenases are exceptions to the biological trend as the metal centers are low spin.

Among the most important reactions of transition metal hydrides are reductive elimination (re) and oxidative addition (oa) of H_2 , which are ubiquitous in organometallic chemistry, including such processes as catalytic asymmetric hydrogenation.¹⁰ The study of these reactions in polynuclear high-spin iron clusters is of particular interest because of mechanistic questions related to the reduction of N_2 to NH_3 by the iron molybdenum cofactor in nitrogenase from *Azotobacter vinlandii*, which has recently been proposed to store reducing equivalents as hydrides that unmask low-valent iron centers upon elimination of H_2 to facilitate binding and reduction of N_2 .⁷ Relatedly, the chemistry of metal hydrides is also germane to chemical hydrogen storage materials for fuel cell applications, in which repetitive cycling between H₂ re and oa are important reactions for discharge and recharging, respectively.¹¹ Ideally, the former would be stimuli-dependent (e.g., reduced pressure, light, exogenous agent) to allow for controlled and on-demand H₂ release. A fundamental understanding of this type of reactivity is thus important to ongoing research efforts, even if transition metal hydrides lack sufficient energy density for use

^aCenter for Catalysis, University of Florida, 214 Leigh Hall P.O. Box 117200, Gainesville, FL 32611, USA. E-mail: murray@chem.ufl.edu

^bDepartment of Chemistry, University of Florida, 214 Leigh Hall P.O. Box 117200, Gainesville, FL 32611, USA

^cDepartment of Chemistry and Biochemistry, University of California San Diego, 9500 Gilman Drive, MC 0358, La Jolla, CA 92093-0358, USA

^dLaboratoire de Chimie de Biologie des Métaux, UMR 5249, Université Joseph Fourier, Grenoble-1, CNRS-CEA 17 Rue des Martyrs, 38054 Grenoble Cedex 9, France

† Electronic supplementary information (ESI) available: Experimental and theoretical procedures and figures, crystallographic details, and theoretical structures. CCDC 1523783 and 1523784. For ESI and crystallographic data in CIF or other electronic format see DOI: 10.1039/c6sc05583d



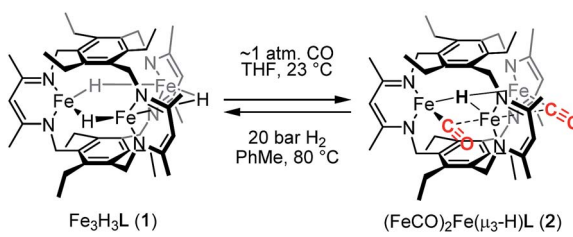
in such applications. Exposure to N_2 , reduced pressure, or visible light irradiation are known to instigate reductive elimination of two hydride donors from transition metal complexes.^{3c,12} In those cases where N_2 is involved, the interplay between N_2 binding and H_2 loss is unclear. Ideally then, compounds that can cycle between H_2 re and oa as a function of a chemical stimulus provide important insight towards tuning the energy demand for discharge and recharge of transition metal hydrides.

We previously reported the synthesis and reactivity of a series of trimetallic trihydride complexes, $M_3(\mu_3\text{-H})_3\text{L}$ ($M = \text{Fe}^{\text{II}}, \text{Co}^{\text{II}}, \text{Zn}^{\text{II}}$), supported by the tris(β -diketiminate)cyclophanate, L^{3-} .¹³ In those reports, we highlighted the surprisingly specific reactivity of these compounds for CO_2 . These metal-hydride compounds were unreactive towards other potential substrates, including nitriles, aldehydes, and ketones. Notably, the Zn^{II} analog demonstrated stability even towards methanol and water. In an effort to expand the substrate scope, we report here the reactivity of $\text{Fe}_3\text{H}_3\text{L}$ (**1**) with carbon monoxide, which resulted in H_2 elimination to generate a formal triiron($\text{I}/\text{II}/\text{II}$) compound, $(\text{Fe}^{\text{I}}\text{CO})_2\text{Fe}^{\text{II}}(\mu_3\text{-H})\text{L}$, and with $\text{BF}_3\cdot\text{OEt}_2$, which afforded $\text{Fe}_3\text{F}_3\text{L}$ through a net fluoride-for-hydride substitution. To our knowledge, the H_2/CO reactivity demonstrated here is the first example of a reversible multielectron redox reaction occurring at a designed high-spin multimetallic compound. Similar reactivity under a minimal driving force is typically invoked as a hallmark of biological catalysis.

Results and discussion

Reaction of **1** with carbon monoxide (~ 1 atm) in THF results in a rapid color change from red to dark yellow-green (broad absorption with $\lambda_{\text{max}} = 320 \text{ nm}$, Fig. S14, ESI \dagger) and formation of $(\text{Fe}^{\text{I}}\text{CO})_2\text{Fe}^{\text{II}}(\mu_3\text{-H})\text{L}$ (**2**) in quantitative yield by ^1H NMR spectroscopy and in good crystalline yield (Scheme 1, 69%). A new resonance corresponding with H_2 is also observed in *in situ* NMR spectra of reaction mixtures, implying H_2 re upon reaction of **1** with CO. This formulation of **2** is supported by single-crystal X-ray diffraction (*vide infra*) and combustion analysis. We also observe a strong IR absorption at 1846 cm^{-1} in spectra of **2** synthesized from ^{12}CO , which shifts to 1804 cm^{-1} for the ^{13}CO labelled **2** ($2\text{-}^{13}\text{CO}$) (theoretical/observed $\Delta\nu(^{12}\text{CO}-^{13}\text{CO}) = 41/42 \text{ cm}^{-1}$).

In the solid-state structure of **2**, two iron centers (Fe2 and Fe3) are in a distorted trigonal pyramidal geometry ($\tau_4 = 0.75$) with each ligated by one semi-bridging CO, one ligand



Scheme 1 Preparation of $(\text{FeCO})_2\text{Fe}(\mu_3\text{-H})\text{L}$ (**2**).

β -diketiminate (or nacnac) arm, and a μ_3 -hydride (Fig. 1, left). The calculated values for α (0.35 and 0.39) and the $\text{Fe}2/\text{Fe}3\text{-C}\equiv\text{O}$ bond angles ($163.7(2)^\circ$ and $162.2(2)^\circ$) agree with Curtis' correlation¹⁴ for bent semi-bridging CO ligands. However, bent $\text{Fe}^{\text{I}}\text{-C}\equiv\text{O}$ bonds are known for terminal carbonyls (*e.g.*, $\sim 173^\circ$ for a (nacnac) $\text{Fe}^{\text{I}}(\text{CO})_2$ complex),^{15a} and the geometric constraints imposed by L^{3-} and $\mu_3\text{H}^-$ likely limit the distance and angular relationships as compared with pseudo-octahedral metal centers. The $\text{Fe}2/\text{Fe}3\text{-N}_\text{L}$ bond distances for **2** are significantly longer than for monometallic nacnac $\text{Fe}(\text{i})$ carbonyls ($>2.05 \text{ \AA}$ *vs.* $1.97\text{--}1.98 \text{ \AA}$),¹⁵ suggesting differing iron spin states or steric effects. The Fe-C bond distances ($1.829(2)$ and $1.830(2) \text{ \AA}$) are within the range of those reported for the (β -diketiminato)iron(i) di- and tri(carbonyl) complexes ($1.79\text{--}1.87 \text{ \AA}$)¹⁵ and for $[\text{PhTp}^{\text{tBu}}]\text{Fe}^{\text{I}}(\text{CO})$ ($1.789(3) \text{ \AA}$)¹⁶ but substantially longer than those reported for Peters' trigonal bipyramidal $\text{Fe}(\text{i})\text{-CO}$ series ($1.679\text{--}1.769 \text{ \AA}$).¹⁷ The energy of $\nu(\text{CO})$ for **2** is also lower than those reported for terminal $\text{Fe}^{\text{I}}\text{-CO}$ species consistent with an interaction with Fe .

Comparison of the Fe-C and C-O bond distances in **2** with those reported for other complexes featuring the monocarbonyl iron motif demonstrates that **2** is atypical with unusually long C-O bonds given the Fe-C bond lengths (Fig. S16–S17 \dagger). We cannot discount libration effects as one reason for the unexpected differences in the bond lengths, although these values are reasonable given the IR data. The (nacnac) $\text{Fe}(\text{H})(\text{CO})$ units in **2** represent the second example of a four coordinate Fe^{I} bearing only one CO donor, the first being $[\text{PhTp}^{\text{tBu}}]\text{Fe}^{\text{I}}(\text{CO})$.¹⁶ The $\text{Fe}(\text{H})(\text{CO})$ fragment is known for P- and N-donor compounds,¹⁸ hydrogenase model compounds,¹⁹ and in metal carbonyl cluster chemistry,⁹ but is unknown for lower than 5-coordinate iron centers. Fe1 is held within a distorted trigonal bipyramidal coordination environment comprising the μ_3 -hydride and two N-atoms from the nacnac arm, and two long axial interactions of $2.481(2) \text{ \AA}$ and $2.545(2) \text{ \AA}$ to the semi-bridging CO donors.²⁰ The bond metrics suggest minimal direct overlap between the iron centers in **2**, which is evident from the formal shortness ratios for the Fe1 contacts (FSR = 1.24 and 1.31).²¹ Specifically, the $\text{Fe}2\text{-Fe}3$ ($3.8612(4) \text{ \AA}$) and $\text{Fe}2/\text{Fe}3\text{-Fe}1$ ($2.9038(5), 3.0428(5) \text{ \AA}$) distances are longer than typically associated with iron–iron bonds. The cyclophane is distorted

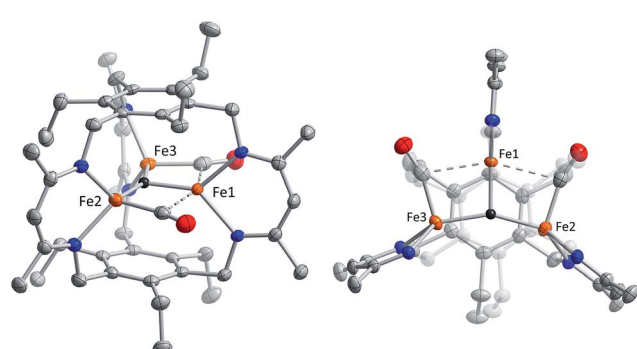


Fig. 1 Solid-state structure of **2** viewed from the side (left) and top (right). C, N, O, and Fe atoms are depicted as grey, blue, red, and orange 75% thermal ellipsoids, and the μ_3 -hydride as a black sphere. All other H-atoms as well as solvent molecules are omitted for clarity.



based on the bond metrics and angles relative to those of the M_3X_3L series ($M = Mn, Fe, Co, Zn, Cu$; $X = Br^-, Cl^-$, and H^-), which highlights the surprising flexibility of L^{3-} .²² The (μ_n -H) Fe_n fragment ($n > 2$) was previously unknown in the high-spin state (*vide infra*), and **2** is the first example of an internal μ_3 -hydride in polyiron chemistry; face-capping μ_3 -hydrides are well-known in iron carbonyl clusters.²³

Reductive elimination of H_2 from **1** should afford a triiron complex with 20 d electrons with formal oxidation states of $Fe^{I_2}Fe^{II}$. This assignment is supported by the zero-field Mössbauer spectrum (Fig. 2), which comprises two different quadrupole doublets with a 2 : 1 area ratio. From the Mössbauer parameters, we assign the doublet with double integration as Fe^I ($\delta = 0.66 \text{ mm s}^{-1}$; $\Delta E_Q = 2.60 \text{ mm s}^{-1}$) and corresponding to $Fe2$ and $Fe3$, whereas the parameters of the other doublet are characteristic of high-spin Fe^{II} ($\delta = 0.98 \text{ mm s}^{-1}$; $\Delta E_Q = 2.15 \text{ mm s}^{-1}$) and attributed to $Fe1$. The δ values assigned to $Fe2$ and $Fe3$ are comparable to those for the high-spin (β -diketiminate)-supported iron(i) complexes with two *tert*-butylisocyanides²⁴ or one dinitrogen bound²⁵ (*c.f.* 0.64 or 0.62, respectively), and distinct from the analogous low-spin iron(i) di- and tri(carbonyl)²⁶ and tris(*tert*-butylisocyanide) compounds (*c.f.* 0.12–0.25).²⁴ This comparison suggests that **2** likely contains high-spin Fe^I centers, which is rare for a CO ligated iron center with tris(pyrazolyl)borate $Fe^I(CO)$ compounds as the only characterized examples.^{16,27} Applying a magnetic field of 2 T at 4.8 K resulted in a slight line broadening for the doublet assigned to Fe^{II} , revealing an internal field of less than 4 T (Fig. S19†). This is indicative of an integer-spin system with a relatively well-isolated $M_S = 0$ ground state within the spin manifold. On the contrary, the doublet assigned to Fe^I is magnetically split between -3 mm s^{-1} and $+4 \text{ mm s}^{-1}$, revealing a much larger internal field. Such behavior excludes the possibility of strongly coupled Fe centers. Consistently, we observe a broad signal near $g = 16$ in X-band EPR spectra collected in parallel mode on **2** (Fig. S13†). Similar spectra are reported for biological and other synthetic polyiron systems and are attributed to weak coupling between integer-spin multiplets.²⁸ As a first approximation, we have simulated the high-field Mössbauer spectra assuming three uncoupled iron centers, two of which account for the two Fe^I centers, with identical

parameters. The overall splittings were well reproduced assuming an $S = 3/2$ ground state for the Fe^I . Additionally, the solution magnetic susceptibility of **2** ($\mu_{eff} = 5.6 \mu_B$) is lower than that of all triiron(ii) complexes supported by L^{3-} (6.2–7.5 μ_B) and is therefore consistent with the $Fe^{I_2}Fe^{II}$ oxidation state assignment.^{13b,35}

The formal metal oxidation state assignments and the overall cofactor charge in the resting state (E_0) of FeMoco remain unclear. Early formulations considered Mo(iv) and various ratios of Fe(ii) and Fe(iii); some of the Fe(ii) and Fe(iii) centers could be treated as mixed-valent pairs (*i.e.*, $2Fe^{2.5+}$).^{29a–e} Currently, the Mo is proposed to be a non-Hund's $S = \frac{1}{2}$ Mo(iii) center based on high-energy resolution fluorescence detected Mo K-edge XAS.^{29f} Spatially resolved anomalous scattering (SpReAD) experiments support the Mo(iii) assignment and suggest an $[Mo^{III}Fe^{II_3}Fe^{III_4}S_9C]^{1-}$ cluster.^{29g} Recent DFT studies by Bjornsson, *et al.* benchmarked to the Mössbauer parameters reported by Yoo, *et al.* are consistent with the SpReAD result or the related isoelectronic mixed-valent formalism (*i.e.*, $[Mo^{III}Fe^{II}Fe^{2.5+}Fe^{III_2}S_9C]^{1-}$).^{29h} Similar ambiguities arise for the one-electron reduced (M^R) and the CO-bound forms of FeMoco, although differences in the experimental conditions (*i.e.*, extracted FeMoco *vs.* holo-MoFe protein) may account for these discrepancies.^{7,29a–c,30} Relatedly, the extent of charge delocalization may be critical to dinitrogen activation. Local iron(i/0) character would be required should N_2 binding and activation by FeMoco parallel synthetic systems.⁴² Our results and the possible coordination number changes for iron center(s) in FeMoco during catalytic turnover^{31,32} hint that these uncertainties should be expected in the reduced states of FeMoco. For example, the isomer shift and quadrupole splittings for $Fe2$ and $Fe3$ could lead to the mistaken assignment of these centers as di-rather than mono-valent, since isomer shifts of 0.66 mm s^{-1} are well within the range of many iron(ii) species.

We previously suggested that loss of H_2 from **1** may be sterically controlled based on the large $H \cdots H$ distances (2.93–3.05 Å).^{13b} H_2 re from **1** is not observed either thermally or under broad wavelength irradiation. For an H_2 re/oa equilibrium to precede CO binding, an H_2 re/oa equilibrium would likely have to exist in which any liberated H_2 reacts rapidly to regenerate **1**, but affords **2** in the presence of high concentrations of CO relative to H_2 (Scheme 2). H_2/D_2 exchange should occur in this mechanism, thereby scrambling the respective isotopic labels. No changes were observed in 1H NMR spectra recorded on reaction mixtures of Fe_3D_3L (**1-D₃**) with H_2 (~1 atm) at temperatures up to 80 °C for 20 h (Fig. S5†). The lack of observable H/D exchange supports CO binding preceding H_2 loss and contrasts the exchange reported for dimeric β -diketiminate complexes.³³ As noted in Scheme 2, we cannot exclude a tightly associated Kubas-type complex between the eliminated H_2 and the triiron species, which does not exchange with dissolved H_2 or D_2 . CO can then coordinate to the Kubas-type species, liberating H_2 and generating **2**. However, such tightly bound M–H₂ complexes on a high-spin metal center are rare,^{11a} and this pathway assumed unlikely. A similar substrate-binding prior to H_2 elimination was recently reported for reaction of a di(μ -hydrido) diiron(ii) complex with diazo compounds.³⁴ In the simplest mechanism, retention of one hydride in **2** would arise from an

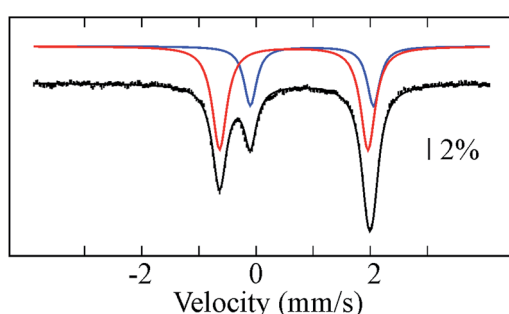
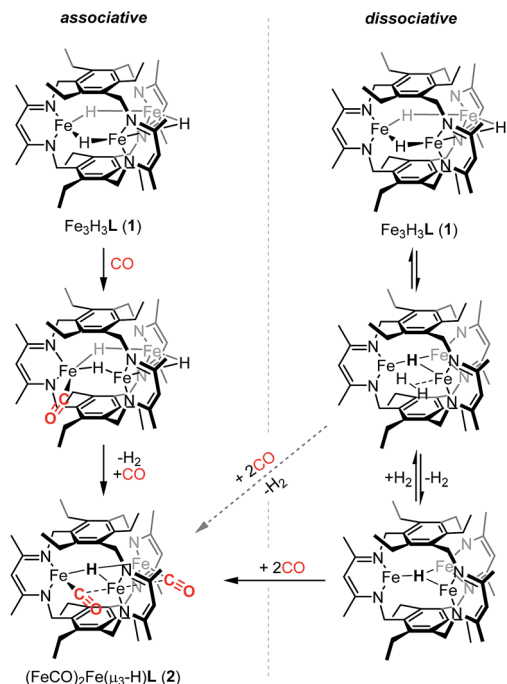


Fig. 2 Mössbauer spectrum of **2** recorded at 80 K and zero-applied field. Black bars and colored lines represent the experimental data points and simulated quadrupole doublets, respectively (Table S1†). Solid black line is a composite spectrum obtained by combining individual doublets.





Scheme 2 Possible associative (left) and dissociative (right) pathways for formation of 2, in which the two pathways can intersect depending on whether H_2 loss succeeds (diagonal dashed arrow) or precedes (horizontal arrow) CO coordination.

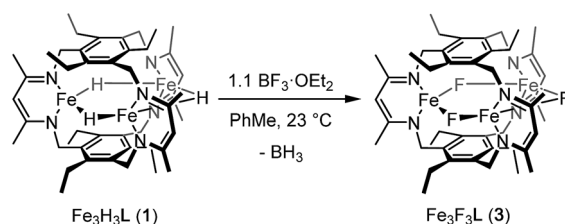
intramolecular step for H_2 loss upon reaction of 1 with CO (Scheme 2). Previously, we provided crystallographic evidence demonstrating that the β -diketiminate and benzene substituents on the ligand for two triiron complexes could interdigitate in the presence of K^+ cations.³⁵ A similar bis(triiron) intermediate could form during H_2 re; however, the predicted long $\text{H}\cdots\text{H}$ distance and the absence of K^+ cations suggests that such an intermediate is also unlikely. Consistent with an intraccluster H_2 re mechanism, we observe only H_2 and not HD in the $^1\text{H-NMR}$ spectra of reactions containing 1 and 1- D_3 under a CO atmosphere (Fig. S7†).

Given that we have hitherto been unable to isolate Fe^{I} -containing complexes for L^{3-} ,³⁵ we were intrigued if reactivity characteristic of Fe^{I} centers could be accessed starting from 2. To that end, we examined the conversion of 2 to 1 upon addition of H_2 . Notably, we observed complete reaction of a toluene solution of 2 with H_2 at 20 bar and 80 °C to yield 1 in 75(7)% spectroscopic yield as a 6.3 : 1 mixture of 1 and an as-yet undetermined decomposition product. Although reversible H_2 re/oa both with and without coordination/dissociation of N_2 are common reactions,^{3c,11a} the reversible H_2 re/oa with CO coordination/dissociation that we observe here is a very rare transformation. Despite the ubiquity of organometallic carbonyls and hydrides, this reaction has been previously reported only for one series of low-spin Group VIII $\text{HM}_3(\text{CO})_9\text{X}$ compounds.³⁶ Because the reactions of mononuclear or self-assembled dinuclear β -diketiminate iron hydrides with CO lead to low-spin polycarbonyl products whose formation is presumably irreversible,^{40b} we hypothesize that our use of a relatively rigid polynucleating ligand is the key factor that enables the unusual

ability to convert between the two species that we observe. Additionally, the interchange between 1 and 2 represents a reversible two-electron redox reaction occurring at a high-spin polyiron cluster, and the starting species 1 demonstrates unusually high substrate specificity.^{13b} As such, the reactivity demonstrated here bears resemblance to the biological reactivity of multimetallic cofactors; the proposed dihydride species in the E_4 state of FeMoco is stable to protonation but readily undergoes reversible re/oa of H_2 . These observations suggest that the bio-inspired design of polynucleating ligands to stabilize high-spin clusters of base metals is a promising strategy for developing base-metal promoted multi-electron chemistry similar to that performed by multimetallic enzymes in biology.

If the dihydrogen reductive elimination is intramolecular, the distance between two hydride donors must necessarily decrease from the solid-state structure of 1 to form H_2 . We posit that CO binds to 1 and stabilizes a structure in which two H^- donors are sufficiently close to liberate H_2 . Fluxional coordination of hydrides³⁷ was proposed in 1 based on our previous reaction study, and a shift of a μ -hydride in 1 towards the internal cavity or to a μ_3 position would generate an open coordination site for CO to bind. With this in mind, we hypothesized that small Lewis acids could coordinate to one or more hydrides in 1 and stabilize such a distorted conformation of $[\text{Fe}_3\text{H}_3]^{3+}$. We probed the reaction of 1 with $\text{BF}_3\cdot\text{OEt}_2$ as others have isolated species with $\text{R}_3\text{B}\cdots\text{H}-\text{M}$ interactions.³⁸ To our knowledge, the $\text{M}-\text{H}\cdots\text{BF}_3$ adduct is rare with the only reported example for a bis(cyclopentadienyl)niobium dihydride.³⁹ We considered, however, the size of the R group and the need for an electron deficient borane in our choice of BF_3 .^{13b}

Reaction of 1 with $\text{BF}_3\cdot\text{OEt}_2$ resulted in formation of a bright yellow solution of $\text{Fe}_3(\mu-\text{F})_3\text{L}$, 3, ($\lambda_{\text{max}} = 321$ nm, 392 nm, 431 nm, Fig. S15†) in near quantitative spectroscopic yield and moderate crystalline yield (Scheme 3, 57%). Our assignment of 3 is supported by combustion analysis, HR-ESI/MS(+), and $^1\text{H-NMR}$; the latter is consistent with a D_{3h} symmetric species in solution and on the method timescale. The solution magnetic susceptibility of 3 is 7.4 μ_{B} ; consistent with that of similar triiron(II) complexes.^{13b,35} The solid-state structure of 3 evidences three bridging fluoride ligands and a planar $[\text{Fe}_3\text{F}_3]^{3+}$ core in 3 (Fig. 3) with comparable bond metrics to related mono- and di-metallic complexes (Table S2†) as well as those in tri-iron(III) and -iron(II) complexes of L^{3-} .^{13b,35,40} Given the quantitative conversion of 1 to 3, the reaction is a net metathesis of $\text{Fe}-\text{H}$ for $\text{B}-\text{F}$ bonds. Consistently, treatment of the reaction mixture with NEt_3 allowed observation of BH_3 as the amine-borane adduct, Et_3NBH_3 , in $^{11}\text{B-NMR}$ spectra. To our knowledge,



Scheme 3 Preparation of $\text{Fe}_3\text{F}_3\text{L}$ (3).

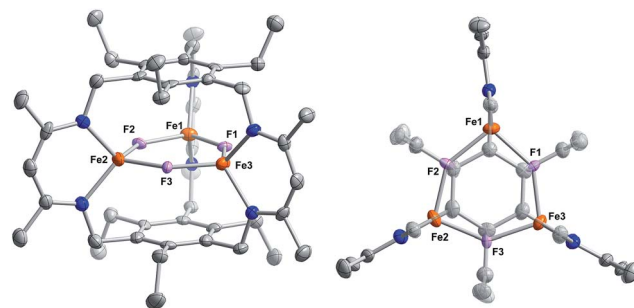


Fig. 3 Solid-state structure of **3** viewed from the side (left) and top (right). C, N, O, F, and Fe atoms are depicted as gray, blue, red, fuchsia, and orange 75% thermal ellipsoids. All H-atoms as well as solvent molecules are omitted for clarity.

this reaction represents the first example of a controlled B–F/Fe–H for B–H/Fe–F bond metathesis. This transformation is enthalpically disfavored (~ 21 kcal mol $^{-1}$ per B–F/Fe–H bond metathesis) based on the average empirical values for the respective bonds.⁴¹ The fact that this reaction proceeds at ambient temperature, however, implies that the bond dissociation energies for the Fe–H and Fe–F bonds in **1** and **3** differ significantly from the reported average empirical values. This deviation from the expected bond enthalpies is likely due to the ligand's unique geometric constraints and the differences in bridging ligand properties of fluoride *versus* hydride. The B–F/Fe–H bond metathesis further illustrates the unexpected reactivity profile of **1** and related trihydride compounds.¹³ Previously, monometallic (nacnac)iron fluoride complexes were reported to react rapidly with trialkylsilanes to generate the corresponding iron hydride complexes.^{40a} However, **3** is unreactive towards the silanes tested based on IR and ^1H -NMR spectroscopy. This reaction should be only slightly enthalpically disfavored relative to the reaction of **1** with BF_3 , but our result is consistent with an unusually large difference between the Fe–F and Fe–H bond strengths in **3** *vs.* **1**. Other factors such as approach of the silyl reagent, access to the transition state geometry, or poor access to the fluoride ligands may also modulate the reaction rate.

Conclusions

We have expanded on the prior reactivity studies reported for **1**, demonstrating that CO triggers reductive elimination of H_2 from **1** to generate an unusual high-spin mixed-valent triiron(I/I $_{\text{II}}$) complex, **2**, and that reaction with $\text{BF}_3\cdot\text{OEt}_2$ affords the tri(μ -fluoride) species **3**. These results add to the growing evidence that hydrides act as effective masks or protecting groups for low-valent high-spin metal centers. In addition, **2** reacts with H_2 to regenerate **1**, which is a rare example of reversible H_2 re/oa involving CO and the first to occur at high-spin metal centers. Ongoing work focuses on continuing to develop the multi-electron reactivity profiles of **1** as well as that of **2**.

Acknowledgements

LJM: University of Florida (UF), ACS Petroleum Research Fund (ACS-PRF 52704-DNI3), National Science Foundation (CHE-1464876, CHE-1048604), J. Goodsell and Prof. A. Angerhofer for help collecting EPR data. RGS: Labex ARCANE (ANR-11-LABX-0003-01). KAA: National Science Foundation (CHE-0821346) and UF for funding of the purchase of the X-ray equipment. KJA: UF University Scholars Program.

1464876, CHE-1048604), J. Goodsell and Prof. A. Angerhofer for help collecting EPR data. RGS: Labex ARCANE (ANR-11-LABX-0003-01). KAA: National Science Foundation (CHE-0821346) and UF for funding of the purchase of the X-ray equipment. KJA: UF University Scholars Program.

Notes and references

- (a) W. Hieber and F. Leutert, *Naturwissenschaften*, 1931, **19**, 360; (b) W. Hieber and H. Schulten, *Z. Anorg. Allg. Chem.*, 1937, **232**, 17.
- (a) *Recent Advances in Hydride Chemistry*, ed. M. Peruzzini and R. Poli, Elsevier, New York, 2001; (b) G. S. McGrady and G. Guilera, *Chem. Soc. Rev.*, 2003, **32**, 383.
- (a) R. Franke, D. Selent and A. Börner, *Chem. Rev.*, 2012, **112**, 5675; (b) M. R. Dubois and D. L. Dubois, *Acc. Chem. Res.*, 2009, **42**, 1974; (c) J. Ballmann, R. F. Munhá and M. D. Fryzuk, *Chem. Commun.*, 2010, **46**, 1013; (d) C. Deutsch, N. Krause and B. H. Lipshutz, *Chem. Rev.*, 2008, **108**, 2916.
- (a) *Ammonia: Catalysis and Manufacture*, ed. A. Nielsen, Springer-Verlag, Berlin, 1995; (b) H.-P. Jia and E. A. Quadrelli, *Chem. Soc. Rev.*, 2014, **43**, 547.
- (a) C. K. Rofer-DePoorter, *Chem. Rev.*, 1981, **81**, 447; (b) M. J. Overett, R. O. Hill and J. R. Moss, *Coord. Chem. Rev.*, 2000, **206**, 581.
- (a) W. Lubitz, H. Ogata, O. Rüdiger and E. Reijerse, *Chem. Rev.*, 2014, **114**, 4081; (b) H. Ogata, K. Nishikawa and W. Lubitz, *Nature*, 2015, **520**, 571.
- (a) B. M. Hoffman, D. Lukyanov, Z.-Y. Yang, D. R. Dean and L. C. Seefeldt, *Chem. Rev.*, 2014, **114**, 4041; (b) D. Lukyanov, N. Khadka, Z.-Y. Yang, D. R. Dean, L. C. Seefeldt and B. M. Hoffman, *J. Am. Chem. Soc.*, 2016, **138**, 1320; (c) D. Lukyanov, N. Khadka, Z.-Y. Yang, D. R. Dean, L. C. Seefeldt and B. M. Hoffman, *J. Am. Chem. Soc.*, 2016, **138**, 10674.
- M. Can, F. A. Armstrong and S. W. Ragsdale, *Chem. Rev.*, 2014, **114**, 4149.
- (a) E. L. Muetterties, R. R. Burch and A. M. Stolzenberg, *Annu. Rev. Phys. Chem.*, 1982, **33**, 89; (b) R. D. Adams and B. Captain, *Angew. Chem., Int. Ed.*, 2007, **47**, 252.
- J. J. Verendel, O. Pàmies, M. Diéguez and P. G. Andersson, *Chem. Rev.*, 2014, **114**, 2130.
- (a) G. J. Kubas, *Chem. Rev.*, 2007, **107**, 4152; (b) B. Sakintuna, F. Lamari-Darkrim and M. Hirscher, *Int. J. Hydrogen Energy*, 2007, **32**, 1121.
- (a) A. S. Weller and J. S. McIndoe, *Eur. J. Inorg. Chem.*, 2007, 4411; (b) R. N. Perutz and B. Procacci, *Chem. Rev.*, 2016, **116**, 8506.
- (a) D. M. Ermert, I. Ghiviriga, V. J. Catalano, J. Shearer and L. J. Murray, *Angew. Chem., Int. Ed.*, 2015, **54**, 7047; (b) Y. Lee, K. J. Anderton, F. T. Sloane, D. M. Ermert, K. A. Abboud, R. García-Serres and L. J. Murray, *J. Am. Chem. Soc.*, 2015, **137**, 10610.
- R. J. Klingler, W. M. Butler and M. D. Curtis, *J. Am. Chem. Soc.*, 1978, **100**, 5034.





15 (a) A. R. Sadique, W. W. Brennessel and P. L. Holland, *Inorg. Chem.*, 2008, **47**, 784; (b) J. M. Smith, A. R. Sadique, T. R. Cundari, K. R. Rodgers, G. Lukat-Rodgers, R. J. Lachicotte, C. J. Flaschenriem, J. Vela and P. L. Holland, *J. Am. Chem. Soc.*, 2006, **128**, 756.

16 J. L. Kisko, T. Hascall and G. Parkin, *J. Am. Chem. Soc.*, 1998, **120**, 10561.

17 (a) S. D. Brown, T. A. Betley and J. C. Peters, *J. Am. Chem. Soc.*, 2003, **125**, 322; (b) C. E. MacBeth, S. B. Harkins and J. C. Peters, *Can. J. Chem.*, 2005, **83**, 332; (c) Y. Lee and J. C. Peters, *J. Am. Chem. Soc.*, 2011, **133**, 4438; (d) J. Rittle and J. C. Peters, *Proc. Natl. Acad. Sci. U. S. A.*, 2013, **110**, 15898.

18 (a) P. Bhattacharya, J. A. Krause and H. Guan, *Organometallics*, 2011, **30**, 4720; (b) N. Gorgas, B. Stöger, L. F. Veiros, E. Pittenauer, G. Allmaier and K. Kirchner, *Organometallics*, 2014, **33**, 6905; (c) E. A. Bielinski, P. O. Lagaditis, Y. Zhang, B. Q. Mercado, C. Würtele, W. H. Bernskoetter, N. Hazari and S. Schneider, *J. Am. Chem. Soc.*, 2014, **136**, 10234.

19 C. Tard and C. J. Pickett, *Chem. Rev.*, 2009, **109**, 2245.

20 Fe1 is disordered in the structure solution: two positions are modelled with minor occupancies of 3.5% and 2.5% (Fig. S18, ESI†). Electron density corresponding to the μ_3 -hydride required partial occupancy of a light atom to model satisfactorily (96% H, 4% O); the contaminant could not be detected by combustion analysis performed on multiple samples of 2.

21 S. J. Tereniak and C. C. Lu, Group 8 Metal-Metal Bonds, in *Molecular Metal-Metal Bonds*, ed. S. T. Liddle, Wiley-VCH, Weinheim, Germany, 2015.

22 (a) G. L. Guillet, F. T. Sloane, D. M. Ermert, M. W. Calkins, M. K. Peprah, E. S. Knowles, E. Čižmár, K. A. Abboud, M. W. Meisel and L. J. Murray, *Chem. Commun.*, 2013, **49**, 6635; (b) Y. Lee, K. A. Abboud, R. García-Serres and L. J. Murray, *Chem. Commun.*, 2016, **52**, 9295; (c) D. M. Ermert, J. B. Gordon, K. A. Abboud and L. J. Murray, *Inorg. Chem.*, 2015, **54**, 9282.

23 (a) C. Femoni, M. C. Iapalucci, G. Longoni, S. Zucchini and S. Zarra, *Inorg. Chem.*, 2009, **48**, 1599; (b) C. Femoni, M. C. Iapalucci, G. Longoni and S. Zucchini, *Dalton Trans.*, 2011, **40**, 8685.

24 S. M. Bellows, W. W. Brennessel and P. L. Holland, *Eur. J. Inorg. Chem.*, 2016, 3344.

25 S. A. Stoian, J. Vela, J. M. Smith, A. R. Sadique, P. L. Holland, E. Münck and E. L. Bominaar, *J. Am. Chem. Soc.*, 2006, **128**, 10181.

26 K. C. MacLeod, D. J. Vinyard and P. L. Holland, *J. Am. Chem. Soc.*, 2014, **136**, 10226.

27 W. H. Harman, Personal communication.

28 (a) M. P. Hendrich, E. Munck, B. G. Fox and J. D. Lipscomb, *J. Am. Chem. Soc.*, 1990, **112**, 5861; (b) H. G. Jang, M. P. Hendrich and L. Que, *Inorg. Chem.*, 1993, **32**, 911; (c) D. P. Goldberg, J. Telser, C. M. Bastos and S. J. Lippard, *Inorg. Chem.*, 1995, **34**, 3011.

29 (a) S. J. Yoo, H. C. Angove, V. Papaefthymiou, B. K. Burgess and E. Münck, *J. Am. Chem. Soc.*, 2000, **122**, 4926; (b) B. Hedman, P. Frank, S. F. Gheller, A. L. Roe, W. E. Newton and K. O. Hodgson, *J. Am. Chem. Soc.*, 1988, **110**, 3798; (c) H.-I. Lee, B. J. Hales and B. M. Hoffman, *J. Am. Chem. Soc.*, 1997, **119**, 11395; (d) R. A. Venters, M. J. Nelson, P. A. McLean, A. E. True, M. A. Levy, B. M. Hoffman and W. H. Orme-Johnson, *J. Am. Chem. Soc.*, 1986, **108**, 3487; (e) T. V. Harris and R. K. Szilagyi, *Inorg. Chem.*, 2011, **50**, 4811; (f) R. Bjornsson, F. A. Lima, T. Spatzal, T. Weyhermüller, P. Glatzel, E. Bill, O. Einsle, F. Neese and S. DeBeer, *Chem. Sci.*, 2014, **5**, 3096; (g) T. Spatzal, J. Schlesier, E.-M. Burger, D. Sippel, L. Zhang, S. L. A. Andrade, D. C. Rees and O. Einsle, *Nat. Commun.*, 2016, **7**, 10902; (h) R. Bjornsson, F. Neese and S. DeBeer, *Inorg. Chem.*, 2017, **56**, 1470.

30 (a) C. J. Pickett, K. A. Vincent, S. K. Ibrahim, C. A. Gormal, B. E. Smith and S. P. Best, *Chem.-Eur. J.*, 2003, **9**, 76; (b) D. Lukyanov, Z.-Y. Yang, D. R. Dean, L. C. Seefeldt and B. M. Hoffman, *J. Am. Chem. Soc.*, 2010, **132**, 2526; (c) P. E. Doan, J. Telser, B. M. Barney, R. Y. Igarashi, D. R. Dean, L. C. Seefeldt and B. M. Hoffman, *J. Am. Chem. Soc.*, 2011, **133**, 17329.

31 T. Spatzal, K. A. Perez, O. Einsle, J. B. Howard and D. C. Rees, *Science*, 2014, **345**, 1620.

32 J. B. Varley, Y. Wang, K. Chan, F. Studt and J. K. Nørskov, *Phys. Chem. Chem. Phys.*, 2015, **17**, 29541.

33 T. R. Dugan, E. Bill, K. C. MacLeod, W. W. Brennessel and P. L. Holland, *Inorg. Chem.*, 2014, **53**, 2370.

34 S. M. Bellows, N. A. Arnet, P. M. Gurubasavaraj, W. W. Brennessel, E. Bill, T. R. Cundari and P. L. Holland, *J. Am. Chem. Soc.*, 2016, **138**, 12112.

35 Y. Lee, F. T. Sloane, G. Blondin, K. A. Abboud, R. García-Serres and L. J. Murray, *Angew. Chem., Int. Ed.*, 2015, **54**, 1499.

36 (a) J. B. Keister, M. W. Payne and M. J. Muscatella, *Organometallics*, 1983, **2**, 219; (b) L. M. Bavaro, P. Montangero and J. B. Keister, *J. Am. Chem. Soc.*, 1983, **105**, 4977; (c) L. M. Bavaro and J. B. Keister, *J. Organomet. Chem.*, 1985, **287**, 357; (d) T. K. Dutta, X. Meng, J. C. Vites and T. P. Fehlner, *Organometallics*, 1987, **6**, 2191.

37 (a) H. D. Kaesz and S. A. R. Knox, *J. Am. Chem. Soc.*, 1971, **93**, 4594; (b) J. Powell, M. R. Gregg and J. F. Sawyer, *J. Chem. Soc., Chem. Commun.*, 1987, 1029.

38 A. Maity and T. S. Teets, *Chem. Rev.*, 2016, **116**, 8873.

39 A. Antiñolo, F. Carrillo-Hermosilla, J. Fernández-Baeza, S. García-Yuste, A. Otero, J. Sánchez-Prada and E. Villaseñor, *J. Organomet. Chem.*, 2000, **609**, 123.

40 (a) J. Vela, J. M. Smith, Y. Yu, N. A. Ketterer, C. J. Flaschenriem, R. J. Lachicotte and P. L. Holland, *J. Am. Chem. Soc.*, 2005, **127**, 7857; (b) Y. Yu, A. R. Sadique, J. M. Smith, T. R. Dugan, R. E. Cowley, W. W. Brennessel, C. J. Flaschenriem, E. Bill, T. R. Cundari and P. L. Holland, *J. Am. Chem. Soc.*, 2008, **130**, 6624; (c) Y. Lee, I.-R. Jeon, K. A. Abboud, R. García-Serres, J. Shearer and L. J. Murray, *Chem. Commun.*, 2016, **52**, 1174.

41 Y.-R. Luo, *Comprehensive Handbook of Chemical Bond Energies*, CRC, Boca Raton, 2007.

42 Selected examples: (a) M. M. Rodriguez, E. Bill, W. W. Brennessel and P. L. Holland, *Science*, 2011, **334**, 780; (b) J. S. Anderson, J. Rittle and J. C. Peters, *Nature*, 2013, **501**, 84; (c) T. J. Del Castillo, N. B. Thompson and J. C. Peters, *J. Am. Chem. Soc.*, 2016, **138**, 5341; (d)

S. Kuriyama, K. Arashiba, K. Nakajima, Y. Matsuo, H. Tanaka, K. Ishii, K. Yoshizawa and Y. Nishibayashi, *Nat. Commun.*, 2016, **7**, 12181; (e) P. J. Hill, L. R. Doyle, A. D. Crawford, W. K. Myers and A. E. Ashley, *J. Am. Chem. Soc.*, 2016, **138**, 13521.

